Micrometric spatial control of rare earth ion emission in $LiNbO_3$: A two-dimensional multicolor array

P. Molina,[1] M. O. Ramírez,[1,a)] J. V. García-Santizo,[1] S. Álvarez-García,[1] R. Pazik,[2] W. Strek,[2] P. J. Dereń,[2] and L. E. Bausá[1]
[1]*Dpt. Física de Materiales, Universidad Autónoma de Madrid, 28049 Madrid, Spain*
[2]*Institute of Low Temperatures and Structure Research, Polish Academy of Science, Okólna 2, 50-950 Wroclaw 2, Poland*

(Received 6 May 2009; accepted 8 July 2009; published online 4 August 2009)

We report on the preparation and optical characterization of a two-dimensional multicolor emission arrangement obtained by embedding high refractive-index Er^{3+} doped $CaTiO_3$ nanoparticles into a Nd^{3+} doped $LiNbO_3$ crystal substrate prepatterned with an array of microvoids. By controlling the spatial location of the rare earth ions at the micrometer scale, we show the possibility of simultaneous spatial and spectral control of the spontaneous emission in a two-dimensional rare earth optically activated array. The results can be useful for the development of microcomposite rare earth based photonic devices, such as multicolor emission displays or pixelated color structures. © *2009 American Institute of Physics*. [DOI: 10.1063/1.3190502]

Manipulating light using patterned structures and materials is central to the current interest in photonic technology. Microstructured optical fibers filled with semiconductors,[1] molecular/hybrid nanoparticle materials,[2] dye-based luminescence microstructures,[3] photonic crystals,[4] or photoluminescent micropatterns in porous silicon[5] constitute representative examples of systems in which patterning gives rise to additional functions useful to control the electromagnetic radiation.

Although an intense activity is nowadays directed toward designing photonic devices by means of a large variety of configurations and materials, the production of organized micro and nanoobjects involving optically active rare earth (RE) ions has been rarely attempted in the past.[6] Our approach to simultaneously control the spatial and spectral light distribution in a wide spectral range is based on the preparation of microluminescent patterns involving optically active trivalent RE^{3+} ions as emitters. Specifically, this work aims at the preparation of ordered luminescent patterns by embedding a high refractive-index material optically activated by RE^{3+} ions into the $LiNbO_3$ nonlinear crystal, also activated by a different RE^{3+}. We show the possibility of a spatial and spectral control of the emission arising from a two-dimensional (2D) pattern useful as a potential multicolor emission array or color display. Further, the work has been performed on an extensively used nonlinear optoelectronic material ($LiNbO_3$), which has demonstrated a large number of applications in integrated optics, such as waveguiding,[7] holographic memories,[8] frequency conversion processes,[9] and the operation as photonic[10] or phononic crystals.[11]

On the other hand, the study of the optical properties of RE^{3+} ion doped materials has constituted an intense research topic and well known applications, such as solid state lasers[12] or phosphors[13] relevant in a good variety of fields, have been developed. Therefore, it seems worthwhile to exploit further the optical properties of RE^{3+} ions in patterned structures with micrometer dimensions. Here, we show the proof of concept of producing 2D multicolor emission patterns by employing the two most extensively used optically active RE^{3+} ions: Er^{3+} and Nd^{3+}. The preparation of organized fluorescent micropattern has been performed by embedding Er^{3+} doped $CaTiO_3$ nanocrystals into a Nd^{3+} doped $LiNbO_3$:MgO monocrystalline substrate on which a microvoid structure was practiced.

To obtain that microvoid structure we have used direct electron beam writing (EBW), without any mask on z-cut Nd^{3+}:$LiNbO_3$:MgO single domain crystals to produce a pattern of polarization inverted domains in the micrometer range. The preparation method is described elsewhere.[14,15] Taking advantage of the different etching rates for domains with opposite polarization, an arrangement of well defined etched-voids was produced after a controlled selective chemical etching on the z^+ face of the substrate. The prepared voids showed a diameter corresponding to the originally inverted domain regions, ranging from 1 to 20 μm. Figure 1(a) shows the scanning electron microscope (SEM)

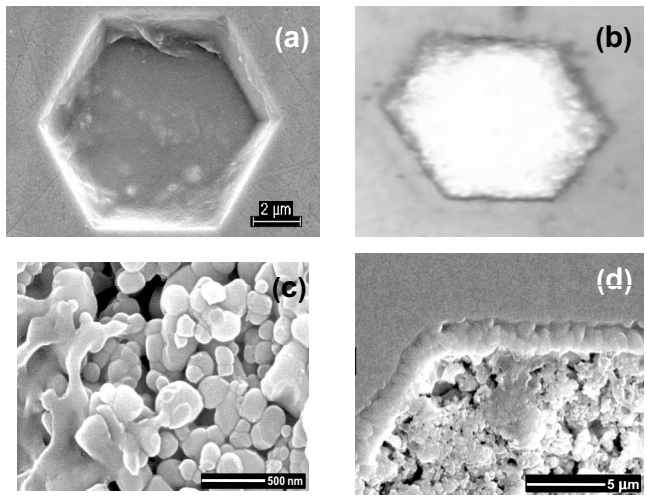

FIG. 1. (a) SEM image of a single hexagonal microvoid in $LiNbO_3$:MgO:Nd^{3+} crystal. (b) Optical micrography of a hexagonal microvoid filled with $CaTiO_3$:Er^{3+} nanocrystals. (c) SEM image of $CaTiO_3$:Er^{3+} nanocrystals into the voids after thermal annealing. (d) Detailed view of a consolidated $CaTiO_3$:Er^{3+}/$LiNbO_3$:MgO:Nd^{3+} microstructure.

a)Electronic mail: mariola.ramirez@uam.es.

 © 2009 American Institute of Physics

Downloaded 04 Sep 2009 to 156.17.85.5. Redistribution subject to AIP license or copyright; see http://apl.aip.org/apl/copyright.jsp

image of a single hexagonal microvoid produced by direct EBW followed by selective chemical etching. The depth of the microvoid is around 3 μm. As observed, the walls and the bottom of the etched microvoid showed a high flatness, as desired for a host cavity. To optically activate those microvoids, Er^{3+} doped $CaTiO_3$ nanoparticles were deposited into them by coating the $LiNbO_3$ substrate with $CaTiO_3:Er^{3+}$ nanopowders and sweeping them across the sample using a scraper. The total spatial extension of the patterns used in this work was 2×2 mm^2. The $CaTiO_3:Er^{3+}$ nanocrystals were prepared by the sol-gel method as described previously.[16] The nanoparticles were checked to be single phased by x-ray diffraction (XRD), which confirmed the presence of orthorhombic $CaTiO_3$ nanocrystals. Er^{3+} concentration in the nanoparticles was 5 at. %. The average particle size was around 50 nm. The election of $CaTiO_3$ as secondary host matrix for RE^{3+} ions was motivated by the attractive properties of perovskite-structure materials in integrated optics and its high refractive index, potentially valuable for light guiding phenomena. In fact, there is a high refractive-index difference between $LiNbO_3$ ($n\sim2.3$) (Ref. 17) and $CaTiO_3$ ($n\sim2.47$ at 500 nm).[18] An optical microscopy image of a hexagonal microvoid filled with $CaTiO_3:Er^{3+}$ is shown in Fig. 1(b). As can be seen, under illumination with white light the pattern resulted in a bright hexagonal area.

The Er^{3+} doped $CaTiO_3$ nanocrystals were consolidated into the voids by means of a thermal treatment at 1000 °C for 2 h. This procedure increased the particle size but preserved the original optical and structural properties of the nanocrystals, as confirmed by XRD and photoluminescence measurements. Figure 1(c) shows a SEM image of the Er^{3+} doped $CaTiO_3$ nanoparticles into the voids after annealing. Though in some regions it is possible to observe particles with their original size (~50 nm), most of them stuck together due to the high temperature required to fix the oxide phosphor into the voids. A view of a corner of the consolidated $CaTiO_3:Er^{3+}/LiNbO_3:MgO:Nd^{3+}$ structure is shown in Fig. 1(d) with a smaller magnification scale. As shown, in addition to the distribution of the optically active $CaTiO_3:Er^{3+}$ nanocrystals inside the etched void, the appearance of a shell (ribbon shaped) is clearly distinguished around the walls. XRD at glazing incidence, as well as spatially resolved confocal micro-Raman spectroscopy, allowed us to identify the compound forming this shell as $CaNb_2O_6$. This compound appears as a result of the reaction of the $CaTiO_3$ nanocrystals with the $LiNbO_3$ substrate at high annealing temperature. Additional information concerning the incorporation of the RE^{3+} ions into the shell, its optical behavior, and impact on the performance of our RE^{3+} activated microluminescent patterns on $LiNbO_3$ are out of the scope of this report and will constitute the subject of a further study.

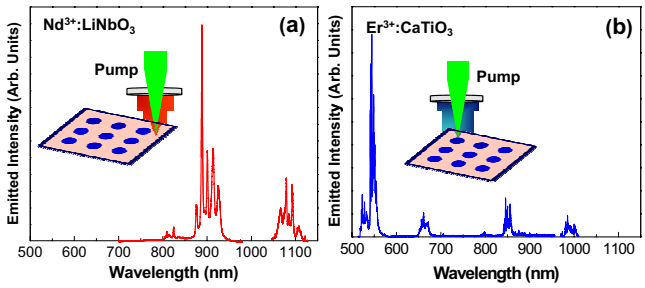

FIG. 2. (Color online) (a) Emission spectrum of the $LiNbO_3:MgO:Nd^{3+}$ substrate collected outside the filled microvoids. (b) Emission spectrum of $CaTiO_3:Er^{3+}$ nanocrystals collected inside a filled microvoid.

To gain further insight into the optical properties of the consolidated structure scanning confocal microfluorescence experiments were performed. Figure 2 shows the emission spectra under excitation at 488 nm when the fluorescence is collected in ($CaTiO_3:Er^{3+}$) and out ($LiNbO_3:Nd^{3+}$) of the filled microvoids. As expected, both systems showed different emission spectra, but with the advantage that they could be recorded under identical excitation conditions. The emission spectrum obtained outside the filled microstructure, i.e., from the $LiNbO_3:MgO:Nd^{3+}$ substrate, consisted mainly of two groups of lines associated with the Stark transitions from the $^4F_{3/2}$ metastable state to the $^4I_{11/2}$ and $^4I_{9/2}$ states of Nd^{3+} ions. Those transitions are peaking at 880 and 1080 nm (laser transition), respectively. The transition from the $^2H_{9/2}$, $^4F_{5/2}$ states to the $^4I_{9/2}$ ground state is also observed at around 815 nm. The spectrum is in good agreement with the reported for the $LiNbO_3:MgO:Nd^{3+}$ laser system.[19]

When the emitted intensity is collected inside the filled microvoid, four main groups of emission lines at 550, 660, 850, and 980 nm, are observed. These groups of lines are related to the radiative de-excitations from the $^2H_{11/2}$, $^4S_{3/2}$, $^4F_{9/2}$, $^4I_{9/2}$, and $^4I_{11/2}$ excited states to the $^4I_{15/2}$ ground state, as well as to the $^4I_{13/2}$ state, of Er^{3+} ions in $CaTiO_3$. The emission spectrum in the 510–560 nm spectral region ($^2H_{11/2}$, $^4S_{3/2}\rightarrow{}^4I_{15/2}$ transition) is shown in Fig. 3(a) with more detail. This spectrum coincides with that previously reported for $CaTiO_3:Er^{3+}$ nanocrystals,[20] indicating that the Er^{3+} emission in $CaTiO_3$ nanocrystals is not altered by the required thermal treatment to consolidate the nanoparticles. Figure 3(b) shows the integrated emission intensity in the green spectral region (510–560 nm) excited and collected across the diameter of a filled microvoid. A large motif ($\sim20\times20$ μm) was chosen to avoid spatial resolution limitations in our experimental conditions. As observed, the emitted intensity shows an almost constant spatial depen-

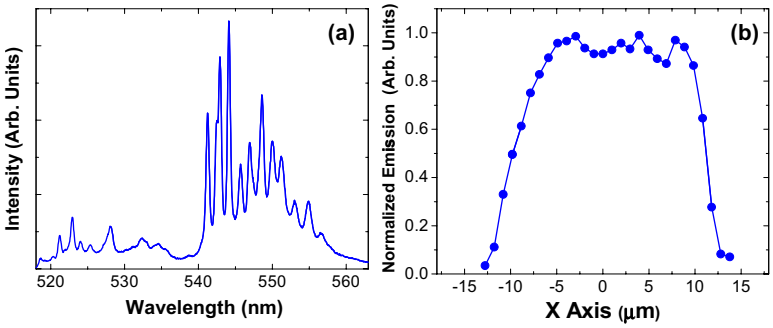

FIG. 3. (Color online) (a) Green luminescence of Er^{3+} doped $CaTiO_3$ nanocrystals embedded in a $LiNbO_3:MgO:Nd^{3+}$ substrate. The emission correspond to the $^4S_{3/2}\rightarrow{}^4I_{15/2}$ and $^2H_{11/2}\rightarrow{}^4I_{15/2}$ transitions of Er^{3+} ions. (b) Integrated emission intensity scanned across the filled microvoid.

Downloaded 04 Sep 2009 to 156.17.85.5. Redistribution subject to AIP license or copyright; see http://apl.aip.org/apl/copyright.jsp

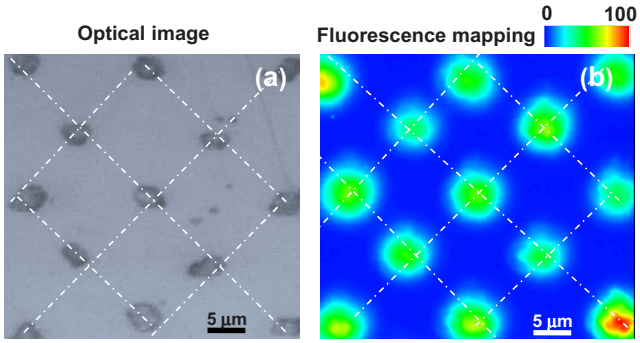

FIG. 4. (Color online) (a) Optical image of a 2D microstructured pattern of $CaTiO_3:Er^{3+}$ nanocrystals into the $LiNbO_3:MgO:Nd^{3+}$ substrate. (b) Spatial luminescent map of the 2D microstructured pattern obtained by integrating the Er^{3+} green emission.

dence, pointing out the good homogeneity in the Er^{3+} distribution in the microvoids.

We would like to remark that under excitation with laser diode at 808 nm the same green emission spectrum ($^2H_{11/2}$, $^4S_{3/2} \rightarrow {}^4I_{15/2}$ transition) was also obtained. In that case, the green emission was produced by means of two-photon mechanisms involving excited state absorption and energy transfer upconversion.[20] Given that Nd^{3+} ions are also efficiently excited at that same wavelength ($^4I_{19/2} \rightarrow {}^2H_{9/2}$, $^4F_{5/2}$ transition) compact optically diode excited devices can be envisaged.

The results in Figs. 2 and 3 clearly shows the feasibility to control the spatial distribution of RE emitters at the microscale by embedding optically active RE^{3+} nanocrystals into a prepatterned substrate. Indeed, it is possible to develop a 2D multicolor emission array based on our composite system. Figure 4(a) shows the optical micrograph of a 2D pattern. It consists of a Nd^{3+} activated $LiNbO_3:MgO$ substrate containing microvoids filled with Er^{3+} doped $CaTiO_3$. The diameters of the voids are around 5 μm and they are periodically separated by a distance of 20 μm forming a square pattern. Figure 4(b) shows the microfluorescence spatial map obtained by integrating the emission spectra in the green spectral region ($^2H_{11/2}$, $^4S_{3/2} \rightarrow {}^4I_{15/2}$ transition). As observed, the fluorescence image is spatially correlated with the $CaTiO_3:Er^{3+}$ areas. Indeed, for the selected spectral range (510–560 nm), only the Er^{3+} filled microvoids contribute to the emitted intensity. Identical spatial emission maps are observed when integrating the Er^{3+} emission in any other band showed on Fig. 2. Moreover, since the $LiNbO_3$ host matrix is optically activated with Nd^{3+} ions, the emitted light from our composite system can be spatially and spectrally switched by exciting and collecting only the fluorescence arising from Nd^{3+} ions into the substrate according to Fig. 2. Thus, the negative image (color reversed) to that of Fig. 4(b) would correspond to the fluorescence map of the emission from Nd^{3+} ions. Additionally, the good variety of excited energy levels of both, Er^{3+} and Nd^{3+} ions, allows switching the pump (excitation) wavelength in such a way that one can selectively excite the filled microvoids, the optically active host matrix, or both systems simultaneously. Moreover, the excitation can be performed on a wide spatial area allowing simultaneous excitation of both, microvoids and host.

In summary, we have shown an example of a 2D patterned multicolor emission array based on the spatial control of optically active RE emitters in the micrometer scale. The work has been carried out on a very interesting nonlinear optoelectronic material, $LiNbO_3$, and allows envisaging RE^{3+} based microcomposite photonic devices from which additional functionalities can be expected. A good variety of physical phenomena can be explored after this work. For instance, radiation confinement and field enhancement into the filled voids, energy transfer processes between different type of active ions which could be affected by the geometry of the composite, or the optical behavior of patterns with different shapes and sizes (namely, submicrometer structures) attainable with the use of the EBW technique.

The authors acknowledge Spanish MICINN under Contract No. MAT2007-64686 and UAM-CM under Contract No. CCG07-UAM/MAT-1861.

[1] P. J. A. Sazio, A. Amezcua-Correa, C. E. Finlayson, J. R. Hayes, T. J. Scheidemantel, N. F. Baril, B. R. Jackson, D.-J. Won, F. Zhang, E. R. Margine, V. Gopalan, V. H. Crespi, and J. V. Badding, Science **311**, 1583 (2006).
[2] N. Gaponik, I. L. Radtchenko, M. R. Gerstenberger, Y. A. Fedutik, G. B. Sukhorukov, and A. L. Rogach, Nano Lett. **3**, 369 (2003).
[3] W. Hu, N. Lu, H. Zhang, Y. Wang, N. Kehagias, V. Reboud, C. M. Sotomayor Torres, J. Hao, W. Li, H. Fuchs, and L. Chi, Adv. Mater. **19**, 2119 (2007).
[4] C. López, Adv. Mater. **15**, 1679 (2003), and references therein.
[5] E. J. Teo, M. B. H. Breese, A. A. Bettiol, D. Mangaiyarkarasi, F. Champeaux, F. Watt, and D. J. Blackwood, Adv. Mater. **18**, 51 (2006).
[6] A. R. Zanatta and C. T. M. Ribeiro, J. Appl. Phys. **96**, 5977 (2004).
[7] P. Becker, R. Brinkmann, M. Dinand, W. Sohler, and H. Suche, Appl. Phys. Lett. **61**, 1257 (1992).
[8] K. Buse, A. Adibi, and D. Psaltis, Nature (London) **393**, 665 (1998).
[9] Y.-C. Huang, A.-C. Chiang, Y.-Y. Lin, and Y.-W. Fang, IEEE J. Quantum Electron. **38**, 1614 (2002).
[10] G. Y. Zhou and M. Gu, Opt. Lett. **31**, 2783 (2006).
[11] M. B. Assouar, B. Vincent, and H. Moubchir, IEEE Trans. Ultrason. Ferroelectr. Freq. Control **55**, 273 (2008).
[12] A. A. Kaminskii, *Laser Crystals: Their Physics and Properties* (Springer, New York, 1981); A. A. Kaminskii, Laser Photonics Rev. **1**, 93 (2007).
[13] W. M. Yen, S. Shionoya, and H. Yamamoto, *Practical Applications of Phosphors* (CRC, Boca Raton, 2006).
[14] P. Molina, D. Sarkar, M. O. Ramírez, J. García Solé, L. E. Bausa, B. J. Garcia, and J. E. Muñoz Santiuste, Appl. Phys. Lett. **90**, 141901 (2007).
[15] P. Molina, M. Ramírez, J. García Solé, and L. E. Bausá, "Effect of electron beam writing parameters for ferroelectric domain structuring $LiNbO_3:Nd^{3+}$," Opt. Mater. (in press).
[16] P. J. Deren, R. Pazik, W. Strek, P. Boutinaud, and R. Mahiou, J. Alloys Compd. **451**, 595 (2008).
[17] G. K. Kitaeva, I. I. Naumova, A. A. Mikhailovsky, P. S. Losevsky, and A. N. Penin, Appl. Phys. B: Lasers Opt. **66**, 201 (1998).
[18] A. Linz and K. Herrington, J. Chem. Phys. **28**, 824 (1958).
[19] R. Burlot, R. Moncorge, H. Manaa, G. Boulon, Y. Guyot, J. Garcia Sole, and D. Cochet-Muchy, Opt. Mater. **6**, 313 (1996).
[20] P. J. Deren, R. Mahiou, R. Pazik, K. Lemanski, W. Strek, and Ph. Boutinaud, J. Lumin. **128**, 797 (2008).

Downloaded 04 Sep 2009 to 156.17.85.5. Redistribution subject to AIP license or copyright; see http://apl.aip.org/apl/copyright.jsp